Available online at www.elixirpublishers.com (Elixir International Journal)

Materials Science

Elixir Materials Sci. 81A (2015) 32073-32079

ISSN: 2229-712X

FT-IR, FT-Raman Spectra and Scaled Quantum Mechanical Study of 5-bromo-2-chlorotoluene

G.Venkatesh[1,*], M.Govindaraju[2] and P.Vennila[3]

[1]Research and Development Centre, Bharathiar University, Coimbatore - 641 046, India.

[2]Department of Chemistry, Kongu Polytechnic College, Erode- 638052, India.

[3]Department of Chemistry, Thiruvalluvar Govt. Arts College, Rasipuram, Tamilnadu, India.

ARTICLE INFO

Article history:

Received: 18 February 2015;

Received in revised form:

5 April 2015;

Accepted: 13 April 2015;

Keywords

Normal Coordinate Analysis,

FT-IR,

Density Functional Theory,

HOMO, LUMO, ESP,

First-order Hyperpolarizability,

Electronic Excitation Energy.

ABSTRACT

The vibrational spectra of 5-bromo-2-chlorotoluene (5B2CT) have been obtained by density functional theory (DFT) calculations. Normal coordinate analysis has been carried out to support the vibrational analysis. The results were compared with the experimental values. With the help of scaling procedures, the observed FTIR and FT Raman vibrational frequencies were analysed and compared with the theoretically predicted vibrational spectra. The assignments of bands to various normal modes of the molecules were also carried out. The Electrostatic potential (ESP) of the title molecule were also performed. Further, density functional theory (DFT) combined with quantum chemical calculations to determine the first-order hyperpolarizability. The calculated HOMO and LUMO energies shows that charge transfer occur within the molecule. Electronic excitation energies, oscillator strength and nature of the respective excited states were calculated by the closed-shell singlet calculation method were also calculated for the molecule.

Introduction

Toluene formerly known as toluol is a clear water-insoluble with the typical smell of paint thinners. Toluene occurs naturally in crude oil and in the tolu tree. It is also produced in the process of making gasoline and other fuels from crude oil and making coke from coal. Toluene is used in making paints, paint thinners, silicone sealants [1], fingernail polish, lacquers, adhesives, and rubber and in some printing and leather tanning processes. The major use of toluene is as a mixture added to gasoline to improve octane ratings. Toluene is also used to produce benzene and as a solvent in paints, coatings, synthetic fragrances, adhesives, inks, and cleaning agents. Toluene is also used in the production of polymers used to make nylon, plastic soda bottles, and polyurethanes and for pharmaceuticals, dyes, cosmetic nail products, and the synthesis of organic chemicals.

Due to toluene interesting characteristics and importance, in the present study we report the vibrational analysis of 5-bromo-2-chlorotoluene (5B2CT) using the SQM force field method based on density functional theory (DFT) calculations. The calculated Infrared and Raman spectra of the title compounds were simulated utilizing the scaled force fields and the computed dipole derivatives for IR intensities and Polaris ability derivatives for Raman intensities.

Experimental Details

The compound 5B2CT was purchased from the Sigma–Aldrich Chemical Company (USA) with a stated purity of greater than 98% and it was used as such without further purification. The FT-Raman spectrum of 5B2CT has been recorded using 1064 nm line of Nd:YAG laser as excitation wavelength in the region 4000-100 cm^{-1} on a Brucker model IFS 66V spectrophotometer equipped with FRA 106 FT-Raman module accessory. The FT-IR spectrum of this compound was recorded in the region 4000–400 cm^{-1} on IFS 66V spectrophotometer.

Computational Details

Quantum chemical calculations were used for 5B2CT to carry out the optimized geometry and vibrational wavenumbers with the GAUSSIAN 09W [2] program using the Becke-3-Lee-Yang-Parr (B3LYP) functional [3,4] supplemented with standard 6-311+G** basis set. The vibrational modes were assigned by means of visual inspection using the GAUSSVIEW program [5]. The symmetry of the molecule was also helpful in making vibrational assignments. The symmetries of the vibrational modes were determined by using standard procedure [6] of decomposing the traces of the symmetry operations into irreducible representations. The prediction of Raman intensities (Ii) were carried out by the following procedure outlined below.

$$I_i = \frac{f(v_o - v_i)^4 S_i}{v_i[1-\exp(-hcv_i/KT)} \quad \text{----------(1)}$$

Where υ_0 is the exciting frequency (in cm^{-1}), υ_i is the vibrational wavenumber of the ith normal mode; h, c and k are fundamental constants, and f is a suitably chosen common normalization factor for all peak intensities.

The Cartesian representation of the theoretical force constant has been computed at the fully optimized geometry by assuming the molecule belongs to C_s point group symmetry. The transformation force field from Cartesian to internal local symmetry coordinates, scaling the subsequent normal coordinate analysis (NCA), calculation of Total Energy Distributions (TED) were done on a PC with the version V7.0-G77 of the MOLVIB program written by Sundius [7].

Results and discussion

Molecular geometry

The molecular structure of the 5B2CT having C_s point group of symmetry is shown in Fig 1. The global minimum

Tele: +91-9965285541

E-mail addresses: venkateshindhuja@gmail.com

energy obtained by the DFT structure optimization was presented in Table 1. The optimized geometrical parameters obtained by the large basis set calculation were presented in Table 2.

Table 1. Total energies of 5B2CT, calculated at DFT B3LYP/6-31G* and B3LYP/6-311+G level**

Method	Energies (Hartrees)
6-31G*	-3302.14755693
6-311+G**	-3302.26739297

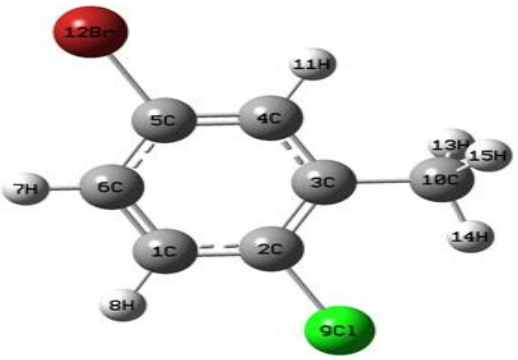

Fig 1. The optimized molecular structure of 5B2CT

Analysis of vibrational spectra

The 39 normal modes of 5B2CT are distributed among the symmetry species as Γ_{3N-6}= 27 A' (in-plane) + 12 A″ (out-of-plane), and in agreement with C_s symmetry. All the vibrations were active both in Raman scattering and Infrared absorption. In the Raman spectrum the in-plane vibrations (A') give rise to polarized bands while the out-of-plane ones (A″) to depolarized band.

Detailed description of vibrational modes can be given by means of normal coordinate analysis (NCA). For this purpose, the full set of 52 standard internal coordinates containing 13 redundancies were defined as given in Table 3. From these, a non-redundant set of local symmetry coordinates were constructed by suitable linear combinations of internal coordinates following the recommendations of Fogarasi et. al [8] are summarized in Table 4. The theoretically calculated DFT force fields were transformed in this later set of vibrational coordinates and used in all subsequent calculations.

The detailed vibrational assignments of fundamental modes of 5B2CT along with calculated IR, Raman intensities and normal mode descriptions (characterized by TED) were reported in Table 5. For visual comparison, the observed and simulated FT-IR and FT-Raman spectra of 5B2CT are produced in a common frequency scales in Fig 2 & Fig 3.

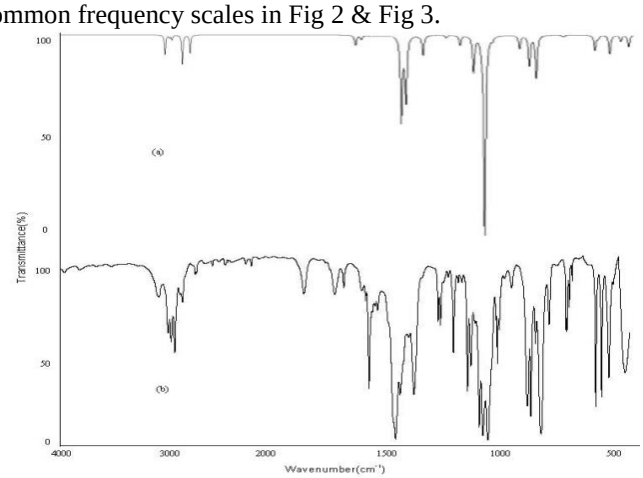

Fig 2. FT-IR spectra of 5B2CT (a) Calculated (b) Observed with B3LYP/6-311+G**

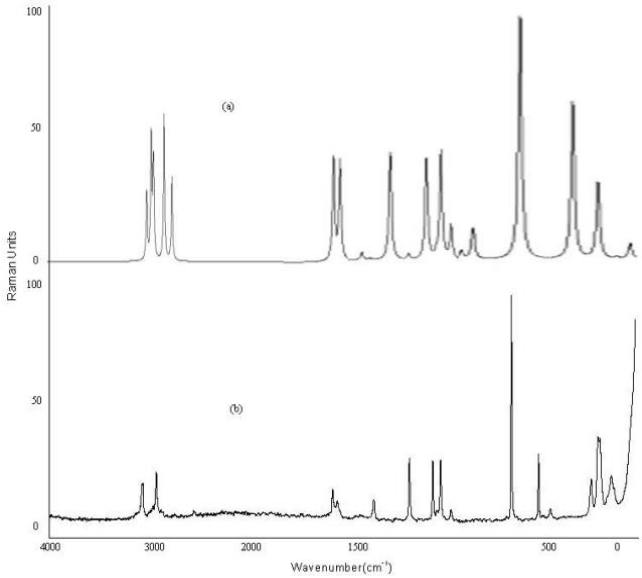

Fig 3. FT-Raman spectra of 5B2CT (a)Calculated (b) Observed with B3LYP/6-311+G**

Root mean square (RMS) values of frequencies were obtained in the study using the following expression,

$$\mathrm{RMS} = \sqrt{\frac{1}{n-1}\sum_{i}^{n}\left(\upsilon_i^{calc} - \upsilon_i^{exp}\right)^2}$$

The RMS error of the observed and calculated frequencies (un scaled / B3LYP/6-311+G**) of 5B2CT was found to be 107 cm^{-1}. This is quite obvious; since the frequencies calculated on the basis of quantum mechanical force fields usually differ appreciably from observed frequencies. In order to reduce the overall deviation between the un scaled and observed fundamental frequencies, scale factors were applied in the normal coordinate analysis and the subsequent least square fit refinement algorithm resulted into a very close agreement between the observed fundamentals and the scaled frequencies. Refinement of the scaling factors applied in this study achieved a weighted mean deviation of 8.81 cm^{-1} between the experimental and scaled frequencies of the title compound.

C–H vibrations

The aromatic structure shows the presence of C-H stretching vibrations in the region 3300–3100 cm^{-1} which is the characteristic region for the ready identification of C-H stretching vibrations [9]. Hence, in the present investigation, the IR and Raman bands at 3238, 3236, 3234, 3191, 3190, 3187 and 3205, 3203, 3202 cm^{-1} in 5B2CT have been designated to C-H stretching vibrations. The C–H out-of-plane deformation vibrations occur in the region 2000–1670 cm^{-1}. This absorption patterns observed at 1647, 1645 and 1640 cm^{-1} for FT-IR and 1617, 1616 and 1614 cm^{-1} for FT-Raman.

C-C vibrations

The ring C-C stretching vibrations, usually occur in the region 1380-1280 and 1625-1435 cm^{-1}. The C-C stretching vibrations of 5B2CT are observed at 1616, 1617, 1614, 1450, 1447 and 1444 cm^{-1} in the FT-IR spectrum and 1433, 1432, 1428, 1307, 1305 and 1302 cm^{-1} in FT-Raman spectrum [10]. These frequencies show that, the substitutions in the ring to some extent about the ring mode of vibrations. The comparison of the theoretically computed values are in good agreement theoretical values obtained by B3LYP/6-311+G** method.

Ring vibrations

Many ring modes are affected by the substitution in the aromatic ring. In the present study, the bands absorbed at 1239,

1238, 1234, 1077, 1070, 1068 and 1061 cm^{-1} in ring in-plane and 967, 965, 964, 910, 908, 905, 837, 835 and 831 cm^{-1} have been designated to ring out-plane modes, respectively.

C–Cl vibrations

In present investigation, The C–Cl stretching frequency is generally observed in the region 800–550 cm^{-1} depending on the configuration and conformation of the compound [11,12]. Based on this, the FT-IR and Raman bands observed at 712, 709, 707, 572, 570, 568, 558, 557 and 554 cm^{-1} has been assigned to C–Cl stretching modes show strong mixing with several planar modes. However, the planar C–Cl bending modes appear to be relatively pure modes. The C–Cl out of plane bending modes were identified at 306, 302, 301 cm^{-1} and 420, 419, 417 cm^{-1} for IR and Raman, respectively.

C–Br vibrations

The vibrations belonging to the bond between the ring and the Bromine atom are important as mixing of vibrations are possible due to the presence of heavy atoms. Bromine compounds absorb strongly in the region 750–530 cm^{-1} due to the C-Br stretching vibrations. In 5B2CT, C–Br stretching and out-of-plane bending modes are recorded at 712, 709 and 707 cm^{-1} in IR. The Raman band at 506, 504 and 502 cm^{-1} is assigned to C–Br in-plane bending vibration.

Methyl group vibrations

The 5B2CT compound, under consideration possesses only one CH_3 group in third position of the ring, respectively. For the assignments of CH_3 group frequencies, one can expect that nine fundamentals can be associated to each CH_3 group, namely the symmetrical (CH_3 ips) and asymmetrical (CH_3 ops), in plane stretching modes (i.e. in-plane hydrogen stretching mode); the symmetrical (CH_3 ss), and asymmetrical (CH_3 ips), deformation modes; the in-plane rocking (CH_3 ipr) out-of-plane rocking (CH_3 opr) and twisting (t CH_3) bending modes. In addition to that, the asymmetric stretching (CH_3 ops) and asymmetric deformation (CH_3 opb) modes of the CH_3 group are expected to be depolarised for A'' symmetry species. The Infrared band found at 3115, 3112, 3111, 3060, 3059 and 3055 cm^{-1} represent symmetric and asymmetric CH_3 stretching vibrations of the methyl group in 5B2CT [13]. The fundamental vibrations arising from symmetric, asymmetric in-plane and out-of-plane deformations, rocking and twisting modes of CH_3 group 5B2CT are observed in their respective characteristic regions and they are listed in Table 5 respectively.

Electrostatic potential

Electrostatic potential (ESP) at a point in space around a molecule gives Information about the net electrostatic effect produced at that point by total charge distribution (electron+ proton) of the molecule and correlates with dipole moments, electro negativity, partial charges and chemical reactivity of the molecules. It provides a visual method to understand the relative polarity of the molecule. An electron density isosurface mapped with electrostatic potential surface depicts the size, shape, charge density and site of chemical reactivity of the molecules.

The electrostatic potential at the surface are represented by different colors; blue represents regions of the most positive electrostatic potential and green represents region of zero potential. Potential decreases in the order green < blue. Such mapped electrostatic potential surface have been plotted for title molecule in B3LYP/6-311+G** basis sets using the computer software Gauss view. Projections of these surfaces along the molecular plane and a perpendicular plane are given in Fig. 4.

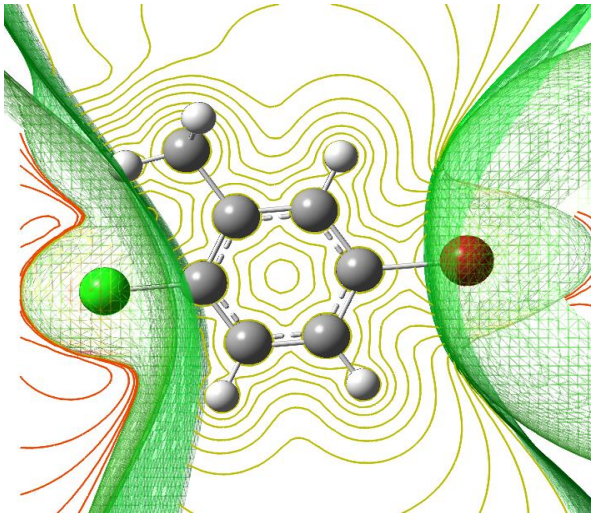

Fig 4. Electrostatic potential surface of 5B2CT

First-order hyperpolarizability calculations

The first-order hyperpolarizibility (β_{ijk}) of the novel molecular system of 5B2CT is calculated using B3LYP/6-311+G** basis set based on finite field approach. Hyper polarizibility is a third rank tensor that can be described by a 3 x 3 x 3 matrix. It strongly depends on the method and basis set used. The 27 components of 3D matrix can be reduced to 10 components due to Kleinman [14] symmetry. It can be given in the lower tetrahedral format. It is obvious that the lower part of the 3×3×3 matrixes is a tetrahedral. The components of β are defined as the coefficients in the Taylor series expansion of the energy in the external electric field. When the external electric field is weak and homogeneous, the expansion becomes

$$E = E^0 - \mu_\alpha F - 1/2\alpha_{\alpha\beta}F_\alpha F_\beta - 1/6\beta_{\alpha\beta\gamma}F_\alpha F_\beta F_\gamma + ...$$

where E^0 is the energy of the unperturbed molecules, F_α the field at the origin μ_α, $\alpha_{\alpha\beta}$, $\beta_{\alpha\beta\gamma}$ are the components of dipole moment, polarizability and the first hyper polarizabilities, respectively. The total static dipole moment μ the mean polarizability α_0 the anisotropy of the polarizability Δα and the mean first hyperpolarizability β_0 using the *x*, *y*, *z* components they are defined as

$$\mu = (\mu_x^2 + \mu_y^2 + \mu_z^2)^{1/2}$$

$$\alpha_0 = \frac{\alpha_{xxx} + \alpha_{yy} + \alpha_{zz}}{3}$$

$$\alpha = 2^{-1/2}[(\alpha_{xx} - \alpha_{yy})^2 + (\alpha_{yy} - \alpha_{zz})^2 + (\alpha_{zz} - \alpha_{xx})^2 + 6\alpha^2 xx]^{1/2}$$

$$\beta_0 = (\beta_x^2 + \beta_y^2 + \beta_z^2)^{1/2}$$

and

$$\beta_x = \beta_x + \beta_{xyy} + \beta_{xzz}$$

$$\beta_y = \beta_{yyy} + \beta_{xyy} + \beta_{xzz}$$

$$\beta_x = \beta_x + \beta_{xyy} + \beta_{xzz}$$

The B3LYP/6-311+G** calculated first hyperpolarizability of 5B2CT is 19.987×10^{-30} esu is shown in Table 6.

Electronic excitation energies, oscillator strength and nature of the respective excited states were calculated by the closed-shell singlet calculation method and are summarized in Table 7. Fig 5. Shows the highest occupied molecule orbital (HOMO) and lowest unoccupied molecule orbital (LUMO) of 5B2CT.

Table 2. Optimized geometrical parameters of 5B2CT obtained by B3LYP/ 6–311+G density functional calculations**

Bond length	Value(Å)	Bond angle	Value(Å)	Dihedral angle	Value(Å)
C2-C1	1.38607	C3-C2-C1	119.99816	C4-C3-C2-C1	0.00000
C3-C2	1.38600	C4-C3-C2	119.99816	C5-C4-C3-C2	0.00000
C4-C3	1.38607	C5-C4-C3	120.00160	C6-C1-C2-C3	0.00000
C5-C4	1.38599	C6-C1-C2	120.00160	H7-C6-C2-C3	-179.00942
C6-C1	1.38599	H7-C6-C2	149.99423	H8-C1-C6-C2	179.42805
H7-C6	1.12197	H8-C1-C6	119.99899	Cl9-C2-C3-C4	-179.42484
H8-C1	1.12204	Cl9-C2-C3	120.00045	C10-C3-C2-C1	-179.42860
Cl9-C2	1.75997	C10-C3-C2	120.00023	H11-C4-C3-C2	-179.42860
C10-C3	1.53998	H11-C4-C3	119.99692	Br12-C5-C4-C3	179.42500
H11-C4	1.12204	Br12-C5-C4	119.99689	H13-C10-C3-C2	119.99843
Br12-C5	1.90997	H13-C10-C3	109.49920	H14-C10-C3-C2	-0.06543
H13-C10	1.12197	H14-C10-C3	109.49750	H15-C11-C3-C2	-119.92683
H14-C10	1.12197	H15-C11-C3	109.50235		
H15-C11	1.12197				

*for numbering of atom refer Fig 1

Table 3. Definition of internal coordinates of 5B2CT

No(i)	symbol	Type	Definition
Stretching 1-6	r_i	C-C	C1-C2,C2-C3,C3-C4,C4-C5,C5-C6,C6-C1
7-9	S_i	C-H	C1-H8,C4-H11,C6-H7
10	p_i	C-Cl	C2-Cl9
11	P_i	C-C(m)	C3-C10
12	ν_i	C-Br	C5-Br12
13-15	n_i	C-H(methyl)	C10-H13,C10-H14,C10-H15
Bending 16-21	α_i	C-C-C	C1-C2-C3,C2-C3-C4,C3-C4-C5, C4-C5-C6,C5-C6-C1,C6-C1-C2
22-27	θ_i	C-C-H	C6-C1-H8,C2-C1-H8,C3-C4-H11, C5-C4-H11,C5-C6-H7,C1-C6-H7
28-29	β_i	C-C-Cl	C3-C2-Cl9, C1-C2-Cl9
30-31	Φ_i	C-C-C	C2-C3-C10, C4-C3-C10
32-33	φ_i	C-C-Br	C4-C5-Br12,C6-C5-Br12
34-36	γ_i	H-C-H	H13-C10-H14,H14-C10-H15,H15-C10-H13
37-39	μ_i	C-C-H	C3-C10-H13,C3-C10-H14, C3-C10-H15
Out-of-plane 40-42	ω_i	C-H	H8-C1-C2-C6,H7-C6-C5-C1, H11-C4-C5-C3
43	ξ_i	C-Cl	Cl9-C2-C1-C3
44	Ω_i	C-C	C10-C3-C2-C4
45	ϖ_i	C-Br	Br12-C5-C4-C6
Torsion 46-51	τ_i	τC-C	C1-C2-C3-C4,C2-C3-C4-C5, C3-C4-C5-C6,C4-C5-C6-C1, C5-C6-C1-C2,C6-C1-C2,C3
52	τ_i	τC-C-H	C2-C3-C10-(H13,H14,H15)

*for numbering of atom refer Fig 1

Table 4. Definition of local symmetry coordinates and the value corresponding scale factors used to correct the force fields for 5B2CT

No.(i)	Symbol[a]	Definition[b]	Scale factors used in calculation
1-6	C-C	r1,r2,r3,r4,r5,r6	0.914
7-9	C-H	S7,S8,S9	0.914
10	C-Cl	p10	0.992
11	C-C(m)	P11	0.992
12	C-Br	ν12	0.992
13	mss	(n13+n14+n15)/ √3	0.992
14	mips	(2n14-n13-n15)/ √6	0.992
15	mops	(n14-n15)/ √2	0.992
16	C-C-C	(α16-α17+α18-α19+α20-α21)/ √6	0.992
17	C-C-C	(2α16-α17-α18+2α19-α20-α21)/ √12	0.992
18	C-C-C	(α17-α18+α20-α21)/2	0.992
19-21	C-C-H	(θ22-θ23)/√2,(θ24-θ25)/√2, (θ26-θ27)/√2	0.916
22	C-C-Cl	(β28-β29)/√2	0.923
23	C-C-C	(Φ30-Φ31)/√2	0.923
24	C-C-Br	(φ32-φ33)/√2	0.923
25	msb	(γ34+γ35+γ36-μ37-μ38-μ39)/ √6	0.990
26	mipb	(2γ36-γ34-γ35)/ √6	0.990
27	mopb	(γ34-γ36)/ √2	0.990
28	mipr	(2μ38-μ37-μ39)/ √6	0.990

29	mopr	(μ37-μ39)/ √2	0.990
30-32	C-H	ω40, ω41, ω42	0.994
33	C-Cl	ξ43	0.962
34	C-C	Ω44	0.963
35	C-Br	ϖ45	0.962
36	tring	(τ46-τ47+τ48-τ49+τ50-τ51)/√6	0.994
37	tring	(τ46-τ48+τ49-τ51)/2	0.994
38	tring	(-τ46+2τ47-τ48-τ49+2τ50-τ51)/√12	0.994
39	C-C-H	τ52/3	0.979

[a] These symbols are used for description of the normal modes by TED in Table 5.
[b] The internal coordinates used here are defined in Table 3.

Table 5. Detailed assignments of fundamental vibrations of 5B2CT by normal mode analysis based on SQM force field calculation

S. No.	Symmetry species C_s	Observed frequency (cm^{-1})		Calculated frequency (cm^{-1}) with B3LYP/6-311+G ** force field				TED (%) among type of internal coordinates[c]
		Infrared	Raman	Unscaled	Scaled	IR[a] A_i	Raman[b] I_i	
1	A'	3238		3236	3234	11.498	74.297	CH(99)
2	A'		3203	3205	3202	1.591	129.878	CH(99)
3	A'	3191		3190	3187	0.687	72.488	CH(99)
4	A'		3188	3187	3184	2.208	42.067	mops(74),mips(24)
5	A'	3112		3115	3111	17.327	142.659	mips(75),mops(24)
6	A'		3060	3059	3055	10.579	77.257	mss(98)
7	A'	1647		1645	1640	5.842	22.893	CC(70),bCH(13),bring(10)
8	A'		1616	1617	1614	2.428	21.538	CC(70),bCH(12),bring(10)
9	A'	1527		1530	1525	49.787	7.217	bmipb(61),bCH(17),CC(11),bmopr(6)
10	A'		1515	1512	1510	7.111	17.711	bmopb(57),bmipb(42)
11	A'			1508	1504	34.908	1.405	bCH(37),CC(34),bmipb(19)
12	A'	1444		1450	1447	0.674	21.563	bmsb(89),CCm(8)
13	A'		1433	1432	1428	11.699	0.937	CC(49),bCH(27),bmipb(5)
14	A'	1333		1335	1331	1.000	1.207	CC(93)
15	A'		1307	1305	1302	1.127	0.238	bCH(76),CC(10)
16	A'	1239		1238	1234	1.501	14.716	CCm(32),CC(30),bCH(24),bring(9)
17	A'		1177	1176	1172	5.754	0.687	bCH(56),CC(33)
18	A'			1115	1111	21.504	11.695	CC(55),bCH(27),CBr(11)
19	A"	1087	1089	1082	1077	3.653	0.518	gCC(39),bmopb(17),bmopr(13),bmipb(13), bmipr(7),tring(6)
20	A'	1070		1068	1061	118.090	11.783	bring(49),CCl(23),CC(16),bmopr(5)
21	A'		1033	1032	1027	2.106	3.479	bmopr(48),CC(22),bmipr(14),bring(9)
22	A"	967		965	964	0.026	0.726	gCH(85),tring(14)
23	A"		908	910	905	7.925	1.752	gCH(79),tring(11)
24	A'	870		863	862	17.818	0.663	bring(43),CCm(24),CBr(17),CC(9)
25	A"	834	837	835	831	25.157	2.293	gCH(88),tring(6)
26	A"			719	715	0.408	0.237	tring(66),gCCl(13),gCC(10),gCBr(7)
27	A"	709		712	707	0.946	14.263	tring(56),CC(16),CCl(14),CBr(6)
28	A'		572	570	568	8.921	6.750	bring(52),CCl(17),CC(11),CCm(11)
29	A"	557		558	554	2.020	0.023	tring(43),gCBr(24),gCC(15),gCCl(14)
30	A'		504	506	502	11.172	2.753	bCC(27),CCl(22),CBr(14),bring(12),bCCl(11)
31	A"			456	452	3.652	0.063	tring(65),gCC(13),gCCl(11),gCH(7)
32	A'	420		419	417	6.929	0.414	bCC(27),bCCl(19),bring(16),bCBr(14),CBr(9),CCl(7)
33	A"		302	306	301	0.196	1.188	gCCl(45),gCBr(21),tring(15),gCC(11),gCH(7)
34	A'			268	263	0.119	5.870	CBr(30),bring(29),bCCl(12),CCl(10),bCC(10),CC(6)
35	A'		257	250	245	1.149	2.769	bCCl(39),bCC(25),CBr(18),bring(8)
36	A"		201	198	196	1.329	2.351	tring(39),gCBr(18),gCC(17),gCH(11),tCH3(11)
37	A'			186	183	0.509	0.274	bCBr(70),bCCl(16),CC(8)
38	A"			149	146	0.441	0.148	tCH3(80),gCC(5)
39	A"			90	88	0.432	0.509	tring(61),gCH(14),gCBr(13),gCCl(7)

Abbreviations used: b, bending; g, wagging; t, torsion; s, strong; vs, very strong; w, weak; vw, very weak;
[a] Relative absorption intensities normalized with highest peak absorption
[b] Relative Raman intensities calculated by Eq 1 and normalized to 100.
[c] For the notations used see Table 4.

Table 6. The dipole moment (μ) and first-order hyperpolarizibility (β) of 5B2CT derived from DFT calculations

β_{xxx}	**-417.35**
β_{xxy}	-8025.7
β_{xyy}	19.786
β_{yyy}	-1219.4
β_{zxx}	97.67
β_{xyz}	3729.3
β_{zyy}	18.42
β_{xzz}	216.53
β_{yzz}	2366.9
β_{zzz}	-37.295
β_{total}	19.987
μ_x	5.2474
μ_y	2.7137
μ_z	0.02500671
μ	0.15838662

Dipole moment (μ) in Debye, hyperpolarizibility $\beta(-2\omega;\omega,\omega)$ 10^{-30}esu.

Table 7. Computed absorption wavelength (λ_{ng}), energy (E_{ng}), oscillator strength (f_n) and its major contribution

n	λ_{ng}	E_{ng}	f_n	Major contribution
1	201.3	6.16	0.0136	H-0->L+0(37%), H-1->L+1(22%), H-1->L+0(20%)
2	196.4	6.31	0.0527	H-0->L+1(+32%), H-1->L+0(26%), H-0->L+0(+22%)
3	186.9	6.63	0.0010	H-0->L+2(+75%)

(Assignment; H=HOMO,L=LUMO,L+1=LUMO+1,etc.)

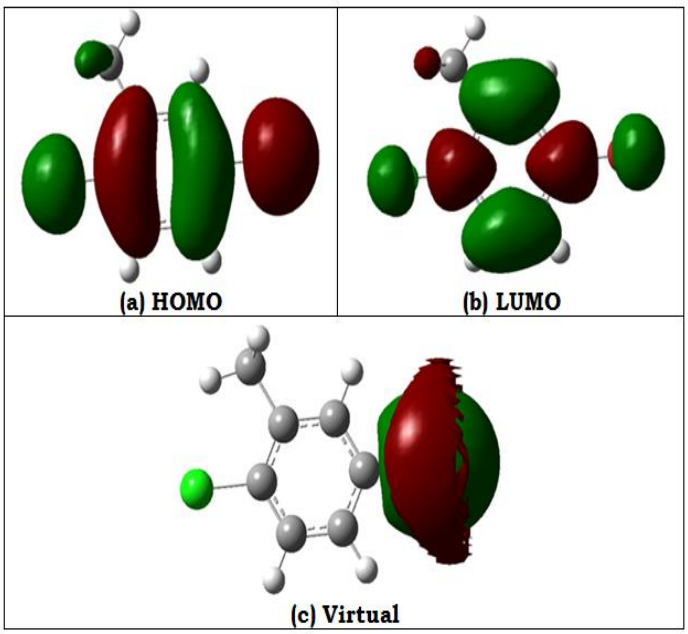

Fig 5. Representation of the orbital involved in the electronic transition for (a) HOMO (b) LUMO (c) Virtual

Orbital involved in the electronic transition for (a) HOMO−0 (b) LUMO+0 (c) HOMO-1 (d) LUMO+1 (e) LUMO+2 is represented in Fig 6. The NLO responses can be understood by examining the energetic of frontier molecular orbitals. There is an inverse relationship between hyperpolarizability and HOMO–LUMO.

HOMO energy = -0.333 a.u

LUMO energy = 0.113 a.u

HOMO–LUMO energy gap = 0.446 a.u

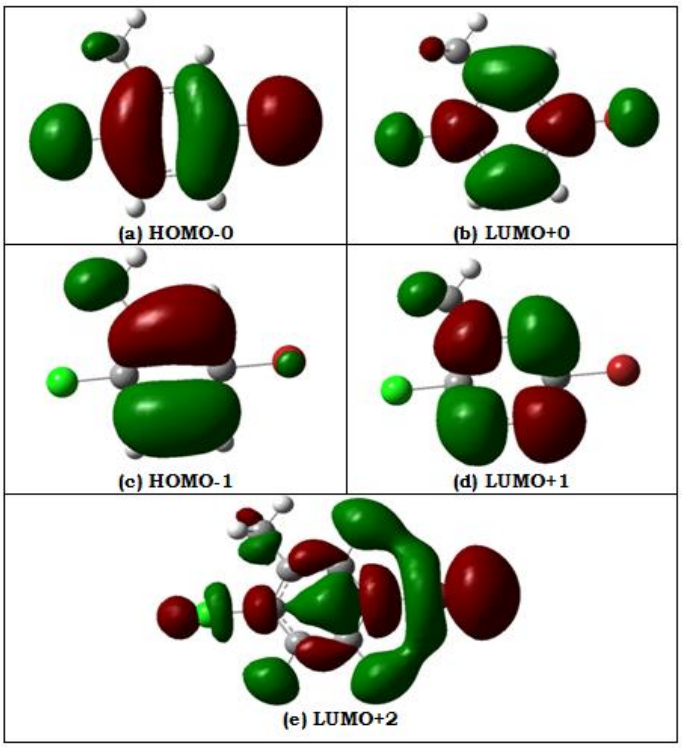

Fig 6. Representation of the orbital involved in the electronic transition for (a) HOMO−0 (b) LUMO+0 (c) HOMO-1 (d) LUMO+1 (e) LUMO+2

Conclusions

FT-IR and FT-Raman Spectra were obtained for 5B2CT, in which bands assigned to 39 normal modes of vibration were observed. A complete vibrational analysis of 5B2CT was performed according to the SQM force field method based on DFT calculations at the B3LYP/6-311+G** levels. The

optimized molecular geometry, force constants and vibrational frequencies were calculated using DFT techniques in the B3LYP/6-311+G** approximation. The resulting SQM force field served to calculate the potential energy distribution, which revealed the molecular vibrations, and the force constants in internal co-ordinates, which were similar to the values obtained before for related chemical species. The electrostatic potential at the surface are represented by different colors; blue represents regions of the most positive electrostatic potential and green represents region of zero potential. The first-order hyperpolarizibility (β_{ijk}) of the novel molecular system of 5B2CT is calculated using B3LYP/6-311+G** basis set based on finite field approach. The calculated first-order hyperpolarizability (β_{total}) of 5B2CT is $19.987x10^{-30}$ esu. Electronic excitation energies, oscillator strength and nature of the respective excited states were calculated by the closed-shell singlet. The NLO responses can be understood by examining the energetic of frontier molecular orbitals. There is an inverse relationship between hyperpolarizability and HOMO–LUMO.

Reference

1. Greenberg, Ronald A, Griswold, Roy M, Lin, Shaow B, Townsend, David F AND Horkay, Ference, Dual cure low-solvent silicone pressure sensitive adhesives, United States Patent, 2002.
2. M. J. Frisch, G. W. Trucks, H. B. Schlegel, G. E. Scuseria, M. A. Robb, J. R. Cheeseman, G. Scalmani, V. Barone, B. Mennucci, G. A. Petersson, H. Nakatsuji, M. Caricato, X. Li, H. P. Hratchian, A. F. Izmaylov, J. Bloino, G. Zheng, J. L. Sonnenberg, M. Hada, M. Ehara, K. Toyota, R. Fukuda, J. Hasegawa, M. Ishida, T. Nakajima, Y. Honda, O. Kitao, H. Nakai, T. Vreven, J. A. Montgomery, Jr., J. E. Peralta, F. Ogliaro, M. Bearpark, J. J. Heyd, E. Brothers, K. N. Kudin, V. N. Staroverov, R. Kobayashi, J. Normand, K. Raghavachari, A. Rendell, J. C. Burant, S. S. Iyengar, J. Tomasi, M. Cossi, N. Rega, J. M. Millam, M. Klene, J. E. Knox, J. B. Cross, V. Bakken, C. Adamo, J. Jaramillo, R. Gomperts, R. E. Stratmann, O. Yazyev, A. J. Austin, R. Cammi, C. Pomelli, J. W. Ochterski, R. L. Martin, K. Morokuma, V. G. Zakrzewski, G. A. Voth, P. Salvador, J. J. Dannenberg, S. Dapprich, A. D. Daniels, O. Farkas, J. B. Foresman, J. V. Ortiz, J. Cioslowski, and D. J. Fox, Gaussian, Inc., Wallingford CT, 2009.
3. A.D. Becke, J. Chem. Phys., 98 (1993) 5648.
4. C. Lee, W. Yang, R.G. Parr, Phys. Rev., B37 (1988) 785.
5. A. Frisch, A.B. Neilson, A.J. Holder, GAUSSVIEW user Manual, Gaussian Inc., Pittsburgh,CT, 2009.
6. P. Venkata Raman Rao, G. Ramana Rao, Spectrochemica Acta Part A 58(2002) 3205−3221.
7. T. Sundius, J. Mol. Struct., 218 (1990) 321.
8. P. Pulay, G. Fogarasi, F. Pong, J.E. Boggs, J. Am. Chem. Soc.,101 (1979) 2550.
9. M.E. Vaschetto, B.A. Retamal, A.P. Monkman, J. Mol. Struct. (Theochem) 468 (1999) 209.
10. T. Chithambarathanu, V. Umayourbagan, V. Krishnakumar, Indian J. Pure Appl. Phys. 40 (2002) 72.
11. S.P. Vijaya Chamundeeswari, E. James Jebaseelan Samuel, N. Sundaraganesan, Spectrochimica Acta Part A: Molecular and Biomolecular Spectroscopy, 110 (2013) 36-45.
12. K. Chaitanya, C. Santhamma, B. Mark Heron, Christopher D. Gabbutt and Alicia C. Instone, Vibrational Spectroscopy, 57 (2011) 35-41.
13. S. Shailajha, U. Rajesh Kannan, S.P. Sheik Abdul Kadhar and E. Isac Paulraj, Spectrochimica Acta Part A: Molecular and Biomolecular Spectroscopy, 133 (2014) 720-729.
14. D.A. Kleinman, Phys. Rev. 1962;126,1977.